CHEMISTRY
A EUROPEAN JOURNAL

DOI: 10.1002/chem.200902470

Lithium Argyrodites with Phosphorus and Arsenic: Order and Disorder of Lithium Atoms, Crystal Chemistry, and Phase Transitions

Shiao-Tong Kong,[a] Hans-Jörg Deiseroth,*[a] Christof Reiner,[a] Özgül Gün,[a] Elmar Neumann,[a] Clemens Ritter,[b] and Dirk Zahn[c]

Dedicated to Professor Dr. Dr. h.c. Arndt Simon on the occasion of his 70th birthday

Abstract: Crystal chemical data of high- (HT) and low-temperature (LT) modifications of lithium argyrodites with the compositions Li_7PCh_6 (Ch = S, Se), Li_6PCh_5X (X = Cl, Br, I), Li_6AsS_5Br, and Li_6AsCh_5I (Ch = S, Se) based on single-crystal, powder X-ray ($113\ K < T < 503\ K$) and neutron measurements ($5\ K < T < 293\ K$) are presented. In the HT modifications, the Li atoms are strongly disordered over a fraction of the available tetrahedral holes, whereas in the LT modifications they occupy ordered crystallographic positions with a pronounced site preference that is analysed on a crystal chemical basis. The Ch/X partial structures remain nearly unchanged upon the reversible phase transitions. Crystal chemical and crystallographic relations between HT and LT modifications based on the Frank–Kasper model of tetrahedral close packing are discussed.

Keywords: argyrodite · crystal engineering · crystal growth · lithium · phase transitions

X-ray single-crystal data for HT-Li_6PS_5I show the electron density of the disordered Li to be smeared out over an extended region preferably inside face-sharing double tetrahedra. A series of temperature-dependent powder neutron data for Li_6PS_5I gives clear evidence for an HT/LT phase transition at ≈ 175 K with an ordering of the Li atoms in different polyhedra with coordination numbers between three and four.

Introduction

A growing number of lithium argyrodites with a dynamic and/or static disorder of Li^+ has been synthesised and characterised recently.[1,2] The chemical compositions of lithium argyrodites can be derived formally by substituting silver in silver argyrodites (e.g., Ag_7PSe_6[3]) by lithium (e.g., Li_7PSe_6). The pronounced disorder of Li^+ in these lithium-rich solids stimulated X-ray-structure and MAS-NMR (magic-angle-spinning NMR) investigations as well as measurements of the Li ionic conductivity, the last studies being currently in progress. All hitherto available data give strong evidence for considerable mobility and Li^+ ionic conductivity in a wide temperature range. The disorder of the Li^+ in these compounds has a remarkable structural background. The three-dimensional arrangement of the chalcogen atoms corresponds to a tetrahedral close packing with an intimate space filling of corner-, edge-, and face-sharing distorted tetrahedra without any other holes in between. In the cubic high-temperature modification (HT) of Li_7PS_6, for example, a small fraction of these tetrahedral holes is occupied by P atoms forming rigid PS_4 tetrahedra, whereas the Li^+ ions are statically/dynamically disordered over the remaining tetrahedral holes. In the corresponding low-temperature (LT) modifications an ordering of the Li^+ ions occurs. For classical Ag and Cu argyrodites many high-temperature (an overview on HT has appeared[4]) but only a few LT modifications could be structurally characterised by X-ray crystallography (e.g., Cu_6PS_5Br[5] (space group *Cc*), Ag_7PSe_6[3] ($P2_13$), Cu_8GeS_6[6] ($Pmn2_1$), Ag_8SiS_6 ($Pna2_1$),[7] Ag_9GaSe_6[8] ($P2_13$)).

[a] S.-T. Kong, Prof. Dr. H.-J. Deiseroth, Dr. C. Reiner, Ö. Gün, Dr. E. Neumann
University of Siegen, Inorganic Chemistry I
Adolf Reichwein Strasse 2, 57068 Siegen (Germany)
Fax: (+49) 271-740-2555
E-mail: deiseroth@chemie.uni-siegen.de

[b] Dr. C. Ritter
Institute Laue Langevin, 6 rue Jules Horowitz
38042 Grenoble Cedex 9 (France)

[c] Dr. D. Zahn
Max Planck Institute for Chemical Physics of Solids
Noethnitzer Strasse 40, 01187 Dresden (Germany)

Supporting information for this article is available on the WWW under http://dx.doi.org/10.1002/chem.200902470.

The presently available experimental results suggest that there are extended structural analogies between the classical Cu and Ag argyrodites and the new Li argyrodites.

In this paper, a comprehensive survey of the present knowledge about Li argyrodites is presented, based on X-ray- and neutron-scattering as well as thermal analyses. This summary includes the occurrence of HT and LT modifications, the conditions of an optimal distribution of the Li^+ ions over the available tetrahedral holes, symmetry relations between HT and LT modifications, apparent suppression of the HT–LT phase transition by partial substitution of chalcogen by halogen and so forth.

Results and Discussion

General remarks: The mineral name "argyrodite" was originally assigned to Ag_8GeS_6[9] in which the element Ge was detected for the first time.[10] Subsequently, reports on a variety of synthetic compounds with a composition that can be derived by substitution of Ge with main group III, IV and V elements and others, by partial substitution of S with other chalcogens or halogens, or by replacement of Ag with Cu have been published. There are also early reports on the replacement of Ag by Cd or Hg (reviewed[4]). A replacement of Ag by Li was not reported. The compounds Li_7PS_6 and Li_7PSe_6 were briefly mentioned together with systematic studies of the systems Li_2Ch to P_2Ch_5 (Ch = S, Se) in three earlier papers;[11–13] however, this was without reference to the argyrodite relationship and without structural information. The first well-defined ternary and quaternary Li argyrodites obtained recently in our group are summarised in Table 1.

These argyrodites are represented by the general formulas Li_7PCh_6 or $Li_{7-\delta}BCh_{6-\delta}X_\delta$ (B = P, As; Ch = S, Se; X = Cl, Br, I; $0 < \delta \leq 1$, dependent on the specific compound). In contrast to the subsequently used crystal chemical analysis of the Li argyrodite structures based on the model of "tetrahedral close packing", the simple ionic description (e.g., Li_7PCh_6 as $7(Li^+)(P^{5+})6(Ch^{2-})$ or Li_6PS_5I as $6(Li^+)(P^{5+})5(S^{2-})(I^-)$) based on the individual coordination polyhedra and their spatial connections gives no information about the chemical background for the disorder and mobility of the Li^+ ions. When one looks closer into the structures, one can recognise that in spite of the differences in composition (e.g., Li_7PCh_6 or $Li_{7-\delta}BCh_{6-\delta}X_\delta$ (B = P, As)), the topology of the atomic arrangements is very similar, and characterised by a replacement of a part of the chalcogen atoms by halogen atoms. For charge balance, the number of Li atoms is reduced accordingly.

It became clear after a number of earlier X-ray structure investigations on silver and copper argyrodites that many if not all argyrodites occur in an HT and at least one LT modification, which is also true for lithium argyrodites. In the cubic HT modification that crystallises in all hitherto known cases in space group $F\bar{4}3m$, the Ch/X atoms occupy the positions of Mg and Cu in the cubic Laves phase $MgCu_2$[14] (Frank–Kasper phase, tetrahedral close packing). Reduced occupancies and pronounced disorder are characteristic for the Ag/Cu atoms. There is a straightforward symmetry relation between the cubic Laves phase and the partial structure of chalcogen atoms in HT argyrodites (Figure 1), which has already been addressed in a general form in an earlier publication.[15]

It is surprising at the first glance that only a minority of structures of the LT modifications of argyrodites has been investigated in detail. It is apparently the occurrence of multiple twinning of crystals upon the phase transitions that complicates detailed structure investigations considerably. Extrapolating, however, from the hitherto known Ag and Cu argyrodite structures, one can predict close relations between Ag/Cu and Li argyrodites with small differences in the Ch/X partial structures. Generally, the low-temperature modification of Ag/Cu argyrodites belong to lower symmetry space groups and are characterised by an ordering of the Ag^+/Cu^+ ions in well-defined coordination polyhedra with fully occupied atomic positions (except β-Cu_7PSe_6[16]). From the results presented in this paper, the same is apparently true for Li argyrodites.

If the composition Li_6PS_5I ($Z = 4$) is referred to as an example, the symmetry relation presented in Figure 1 must be seen against the background that in the cubic unit cell of the HT modification 20 sulfur and four iodine atoms (Li_6PS_5I, I = "S3") are present. The partial structure of these 24 atoms forms 136 distorted tetrahedral holes that are intimately connected through common corners, edges, and faces ("tetrahe-

Table 1. Summary of crystal data of synthetic lithium argyrodites.

Phase	Space group, lattice constants [Å]	Ref.
HT-Li_7PS_6[a]	$F\bar{4}3m$, $a = 9.9926(12)$ ($T = 503$ K)	[d]
HT-Li_7PSe_6[a]	$F\bar{4}3m$, $a = 10.4752(12)$ ($T = 453$ K)	[d]
LT-Li_7PS_6[b]	$Pna2_1$, $a = 14.076(6)$, $b = 6.917(2)$, $c = 9.955(4)$	[d]
LT-Li_7PSe_6[b]	$Pna2_1$, $a = 14.760(2)$, $b = 7.270(8)$, $c = 10.448(2)$	[d]
HT-$Li_{7-\delta}PS_{6-\delta}Cl_\delta$[a]	$F\bar{4}3m$, $a = 9.859(2)$, $\delta < 1$	[1]
HT-$Li_{7-\delta}PS_{6-\delta}Br_\delta$[a]	$F\bar{4}3m$, $a = 9.988(2)$, $\delta = 0.75$	[1]
HT-Li_6PS_5I[a]	$F\bar{4}3m$, $a = 10.1448(16)$	[1]
LT-Li_6PS_5I[c]	Cc, $a = 12.3217(4)$, $b = 7.1377(3)$, $c = 12.4490(4)$ $\beta = 109.481(3)°$ ($T = 170$ K)	this work
HT-$Li_{7-\delta}PSe_{6-\delta}Cl_\delta$[a]	$F\bar{4}3m$, $a = 10.3620(10)$, $\delta = 0.31$	this work
HT-$Li_{7-\delta}PSe_{6-\delta}Br_\delta$[b]	$F\bar{4}3m$, $a = 10.3804(3)$, $\delta < 1$	this work
HT-$Li_{7-\delta}PSe_{6-\delta}I_\delta$[a]	$F\bar{4}3m$, $a = 10.5400(10)$, $\delta = 0.75$	this work
HT-$Li_{7-\delta}AsS_{6-\delta}Br_\delta$[a]	$F\bar{4}3m$, $a = 10.102(1)$, $\delta = 0.98$	this work
HT-Li_6AsS_5I[a]	$F\bar{4}3m$, $a = 10.237(1)$	this work
LT-Li_6AsS_5I[b]	Cc, $a = 12.388(3)$, $b = 7.285(3)$, $c = 12.485(3)$, $\beta = 109.7(5)°$ ($T = 113$ K)	this work
HT-Li_6AsSe_5I[a]	$F\bar{4}3m$, $a = 10.652(1)$	this work

[a] Single crystal. [b] Powder. [c] Rietveld from neutron powder data. [d] Publication in progress.

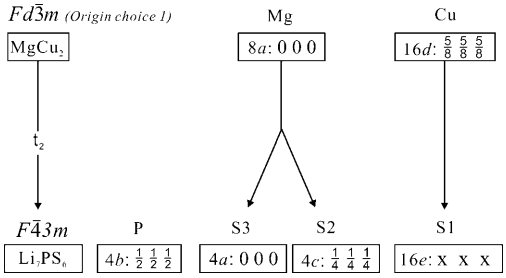

Figure 1. Symmetry relations between the atomic positions of Mg and Cu in the cubic Laves phase $MgCu_2$ and the distribution of chalcogen atoms in HT-Li_7PCh_6. Due to two possible origin choices for $Fd\bar{3}m$ and two possible structure settings for space group $F\bar{4}3m$ (non-centric, absolute configuration), the literature notations for the atomic positions of argyrodite structures are somewhat inconsistent.

Table 2. Possible settings of atomic coordinates for the two origin choices and the corresponding inverted structures of HT argyrodites crystallising in the space group $F\bar{4}3m$. (The **bold** entries show the Wyckoff positions for inverted structure change.)

Atom	Wyckoff position	*x*	*y*	*z*	Wyckoff position	*x*	*y*	*z*
		Setting 1				Setting 1 inverted		
P	**4*d***	**3/4**	**3/4**	**3/4**	**4*c***	**1/4**	**1/4**	**1/4**
Ch1	16*e*	≈7/8	≈7/8	≈7/8	16*e*	≈1/8	≈1/8	≈1/8
Ch2	4*b*	1/2	1/2	1/2	4*b*	1/2	1/2	1/2
Ch3	**4*c***	**1/4**	**1/4**	**1/4**	**4*d***	**3/4**	**3/4**	**3/4**
		Setting 2				Setting 2 inverted		
P	4*b*	1/2	1/2	1/2	4*b*	1/2	1/2	1/2
Ch1	16*e*	≈5/8	≈5/8	≈5/8	16*e*	≈3/8	≈3/8	≈3/8
Ch2	**4*c***	**1/4**	**1/4**	**1/4**	**4*d***	**3/4**	**3/4**	**3/4**
Ch3	4*a*	0	0	0	4*a*	0	0	0

dral close packing"). There are no other holes. The four P atoms per unit cell occupy four such tetrahedra, forming rigid PS_4 groups without direct connection to each other. Basically, the 24 Li atoms could be distributed over the remaining 132 tetrahedral holes in a statistical way (for restrictions, see below). MAS-NMR[1] and electrochemical impedance measurements currently in progress support the structural findings of a dynamic disorder of the Li^+ ions at higher temperatures.

As mentioned above, the X-ray structure refinements of Li argyrodites are characterised by apparent problems that are more pronounced than in classical Ag/Cu argyrodites, in which in some cases even the sensitive refinement of anharmonic temperature parameters for Ag^+/Cu^+ in HT argyrodites was possible.[3] Due to the low scattering power of Li, this is impossible for HT-Li argyrodites. Information on the Li^+ ordering in the LT modifications suffer mainly from the fact that only powder samples are available up to now, because the phase transition is inevitably associated to the formation of multiple twins.

Suitability of tetrahedral holes for occupation by Li^+: When comparing published HT structures of argyrodites, one should be aware of origin settings differing by $^1/_2$, $^1/_2$, $^1/_2$. Together with a possible inversion of the atomic positions, the P or equivalent atoms are located either in Wyckoff position 4*b*, 4*c*, or 4*d* of space group $F\bar{4}3m$ (No. 216). This has also consequences for Wyckoff positions of several other atoms and centre positions of empty/filled tetrahedral holes. A summary of the four possible settings for the Wyckoff positions of P and Ch (neglecting Li/Ag/Cu) is given in Table 2.

The most important aim of the subsequent crystal chemical analysis is a rationalisation of the suitability of the different types of tetrahedral holes for an occupation by disordered/ordered Li atoms in the HT/LT phase.

A systematic analysis of the 136 tetrahedral holes per unit cell shows that the holes can be classified into different types (Table 3). In HT-Li_7PS_6, type 0 (4*b*) is occupied by P atoms forming rigid PS_4 groups, thus reducing the number of tetrahedral holes available for Li from 136 to 132. At a first glance one would expect all remaining 132 tetrahedral holes to be of similar suitability for an occupation by Li atoms. This, however, is not the case. It is apparently the criterion of how many common corners, edges, or faces the referenced tetrahedron type shares with the rigid PS_4 tetrahedra that determines whether the referenced tetrahedron is suitable or unsuitable for Li^+. In particular, type 1 tetrahedra are completely unsuitable for occupation by Li atoms, because they share common faces with PS_4 groups and thus strong repulsive interactions between Li and P atoms are to be expected ($d_{P-Li} \approx 150$ pm, Figure 2). A similar but weaker

Table 3. Crystal chemical analysis of the 136 tetrahedral holes formed by the S atoms in the unit cell of HT-Li_7PS_6 ($F\bar{4}3m$, origin setting 2, see Table 2). The suitability criteria refer to the hypothetic Li atoms located in (or near) the centre of the particular tetrahedron type (Wyckoff notation of centre position in column 2) and the question of how many common corners, edges, or faces the pertinent tetrahedron type share with the rigid PS_4 tetrahedra. Although not a tetrahedron centre, the important position 5a is listed (see text for details).

Type	Wyckoff notation for tetrahedron centre (special: type 5*a*)	Suitability of the pertinent position for occupation by Li^+
0	4*b* (P)	unsuitable: blocked by fixed P atoms forming rigid PS_4 tetrahedron
1	16*e*	unsuitable: common faces with PS_4 tetrahedra
2	48*h*	restricted suitability: common edges with PS_4 tetrahedra
3	4*d*	suitable: four common corners with neighboring PS_4 tetrahedra (no common edge)
4	16*e*	suitable: three common corners with three neighboring $PS(1)_4$ tetrahedra
5	48*h*	suitable: two common corners with neighboring PS_4 tetrahedra only, face-sharing double tetrahedra
trigonal planar position		
5a	24*g*	*important position* located in the centre of the common face of two type 5 tetrahedra, CN = 3, trigonal planar

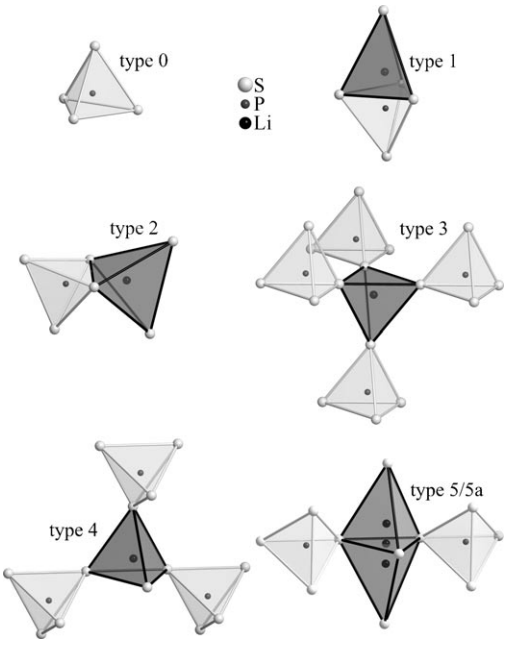

Figure 2. Simplified representation of the tetrahedron types 1–5 (dark gray) with respect to their orientation relative to the PS_4 groups (type 0, light gray). The trigonal planar position 5a is located in the common face of two type 5 tetrahedra.

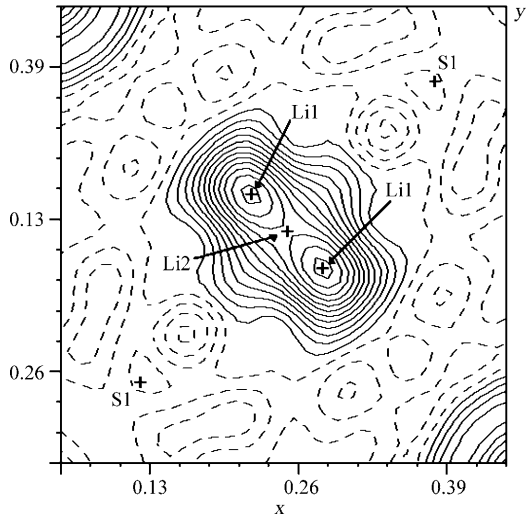

Figure 3. Fourier section ($z = 0.54$) for Li_6PS_5I showing the electron density associated with type 5 double tetrahedra (48*h*, Li1) and type 5a trigonal planar coordination (24*g*, Li2) (Fourier coefficients based on a refinement without Li, resolution 0.1 Å, contour interval 0.1 e $Å^{-3}$).

argument holds for type 2 tetrahedra because of common edges with PS_4 groups. Type 3, 4, and 5 tetrahedra are suitable for occupation with disordered/ordered Li from crystal chemical arguments because they share corners only with PS_4 tetrahedra. In particular, type 5 tetrahedra are highly suitable for Li atoms, because they only share two common corners with neighboring PS_4 tetrahedra. This tetrahedron type is 48-fold and represents locally the two centres of a face-sharing double tetrahedron. Because of the short interatomic distances between the two, only one of them can be occupied at the same time, thus representing only 24 atoms per unit cell. In this context, type 5a is very important. It is located in the common trigonal planar face of a type 5 double tetrahedron representing a trigonal planar coordination. Indeed, more or less pronounced "smeared out" electron densities including the type 5 and 5a positions (but generally not centred at 5a) are observed for all HT modifications of argyrodites (Figure 3).

Moreover non-occupation of type 5 or 5a with Li atoms reduces the reliability factor in X-ray single-crystal structure refinements of HT Li argyrodites significantly, and this is a strong indication for the physical reality of electron density in this position. One can simulate the related electron density distribution (Figure 3) by a split position (Li1, 48*h*) with a density maximum on both sides of the triangular face or, less effectively, by a single position (Li2, 24*g*). Because in both cases a maximum of 24 Li atoms per unit cell can only occupy this region of the structure (see above), the argyrodites with a composition such as Li_6PCh_5X ($Z = 4$, 24 Li per unit cell) just fulfill this condition, but those with the composition Li_7PCh_6 ($Z = 4$, 28 Li) do not. Interestingly, in LT modifications of argyrodites with the composition M_6PCh_5X, it is either the type 5a or one of the two type 5 positions (i.e., corresponding positions in the lower symmetric space group) that is occupied by Li/Ag/Cu atoms in an ordered way. Only in argyrodites with more than six M atoms per formula unit ("excess Li" in, e.g., Li_7PS_6) the M atoms have to occupy further, less suitable atomic positions (see below) in the tetrahedral framework.

It is common to most LT modifications that the M atoms are either partly or completely frozen out in three types of specific positions (Figure 4) in the tetrahedral framework of

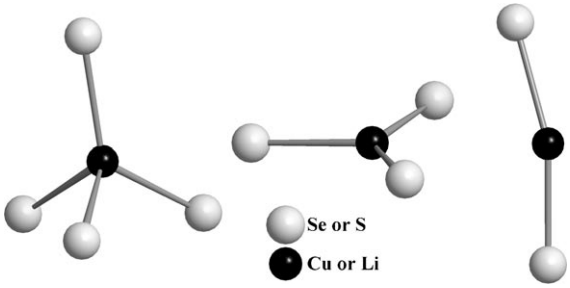

Figure 4. First-sphere coordination polyhedra of ordered Li^+ in LT-Li_7PCh_6 (5 × tetrahedral, 1 × trigonal, 1 × "linear"). All positions are located in the centre, a face or an edge of a type 5 double tetrahedron.

Ch/X atoms: 1) centre or near centre positions (type 5) of tetrahedra, 2) centre or near centre positions of common triangular faces of type 5 double tetrahedra (type 5a), and 3) positions on edges of tetrahedra (e.g., common edge of three type 5 double tetrahedra) with linear or nearly linear twofold coordination.

The preceding suitability classification of the tetrahedral holes is basically confirmed by molecular dynamics calculation for Li_7PS_6 (Table 4). There is a slight discrepancy regarding the sequence of the type 3 and 4 tetrahedra. Concerning the results for Li_6PS_5I, it should be noted that this compound contains S_4 and mixed S_3I tetrahedra.

Table 4. Free enthalpies of different Li sites in Li_7PS_6 and Li_6PS_5I as derived from Boltzmann statistics on the basis of constant pressure and constant temperature molecular dynamics simulations. In Li_6PS_5I, types 5, 4, and 2 represent S_3I tetrahedra, and types 3 and 1 represent S_4 tetrahedra.

Type	Free enthalpy [eV] Li_7PS_6	Free enthalpy [eV] Li_6PS_5I
5/5a	0	0
4	0.24	0.14
3	0.22	0.39
2	0.32	0.27
1	unoccupied	unoccupied

HT- and LT-Li_7PCh_6 (Ch=S, Se): The X-ray single-crystal structures of the HT and LT modifications of these halide-free Li argyrodites (publication currently in progress) clearly demonstrate that they crystallise in space group $F\bar{4}3m$ isotypic to all known HT structures of argyrodites.

Experimental data available up to now give strong evidence that the LT modifications of this composition type crystallise isotypical to α-Cu_7PSe_6[17] (orthorhombic space group $Pna2_1$). A tree of symmetry describing the relationship between the HT modification and possible space groups for the LT modifications was already published earlier.[15]

HT-$Li_{7-\delta}PCh_{6-\delta}X_\delta$ (Ch=S, Se, X=Cl, Br, I): A general description of the HT modifications of this group of halide-containing Li argyrodites with Ch=S, Se and X=Cl, Br, I has appeared previously.[1] X-ray and MAS-NMR results prove clearly that Li_6PS_5I is the only example in which halogen(I) and chalcogen atoms occupy separate crystallographic positions. In all other Li argyrodites of this type, chalcogen and halogen atoms share at least two common crystallographic positions randomly. Thus a formulation $Li_{7-\delta}PCh_{6-\delta}X_\delta$ ($\delta \leq 1$) is more appropriate, because the random substitution of chalcogen by halogen concerns Ch3 as well as Ch2; Ch1 is directly bonded to P and is not affected significantly by the substitution.

The general crystal data of the quaternary HT argyrodites (Table 1) are very similar to those of the corresponding ternary ones, except for a small but significant difference in the lattice constants, which is in accordance with the sequence of ionic radii for the respective Ch^{2-} and X^- ions.

Although the X-ray single-crystal structure data for HT modifications of these Li argyrodites are only weakly significant with respect to the Li positions, a summation of the delocalised electron densities around holes of type 5 and 5a comes surprisingly close to the theoretical value of 24 Li atoms per unit cell.

LT-$Li_{7-\delta}PCh_{6-\delta}X_\delta$ (Ch=S, Se, X=Cl, Br, I): An important aspect of this group of argyrodites is the apparent lowering of the HT–LT transition temperature (T_t) in comparison to the halide-free compounds. For the pair Li_7PS_6/Li_6PS_5I, the transition temperature is reduced from 483 K to 173 K. For most other halide-containing compounds (except Li_6AsS_5I, see below) we could not detect a transition even when cooling down to 113 K. Although not proven in general, it seems that any substitution in the ternary Li argyrodites lowers the HT–LT transition temperature significantly, because for the mixed crystal series $Li_7PS_{6-x}Se_x$ ($0 \leq x \leq 6$), T_t also goes through a minimum for $x \approx 3$ (publication currently in progress).

Owing to the already mentioned multiple twinning upon the HT–LT phase transition and the low transition temperatures T_t for Li_6PS_5I, the available structure information is based on powder X-ray and neutron diffraction data only. A series of low-temperature neutron powder diagrams for Li_6PS_5I confirms the phase transition (Figure 5 and Supporting Information).

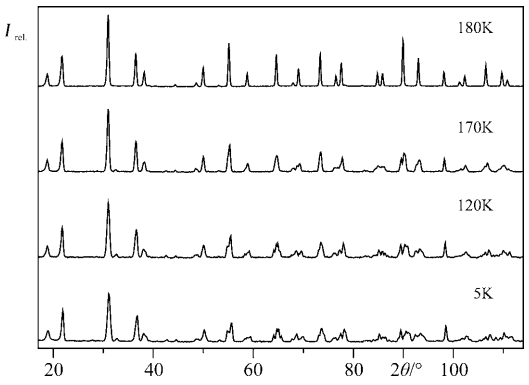

Figure 5. Sections of neutron powder diagrams of Li_6PS_5I at different temperatures. The phase transition takes place between 170 and 180 K ($\lambda = 1.91$ Å, instrument D1A).

The powder neutron and X-ray data give strong evidence that LT-Li_6PS_5I is crystallised isotypically with the monoclinic LT-Cu_6PS_5Br.[5] Figure 6 demonstrates clearly the close relationship between the HT and LT structure resulting in a monoclinic (pseudocubic) unit cell for LT-Li_6PS_5I. (Additionally, the relationship between the orthorhombic LT-Li_7PCh_6 and HT-Li_7PCh_6 type is shown.)

A Rietveld plot for the refinement of the 170 K neutron powder data based on starting parameters taken from LT-Cu_6PS_5Br is presented in Figure 7. Summaries of important crystallographic data and refinement parameters are given in Tables 5–7.

The six crystallographically independent Li atoms occupy 3×T5 (tetrahedral position, Li3, Li4, Li6; see Table 7) and 3×T5a (trigonal position, Li1, Li2, Li5) positions in an ordered way (see Figure 8, middle). In contrast to the Cu compound, the Li atoms in T5a show a significant tendency to leave the trigonal planar position (for distances, see Supporting Information). Possibly, this behaviour reflects the

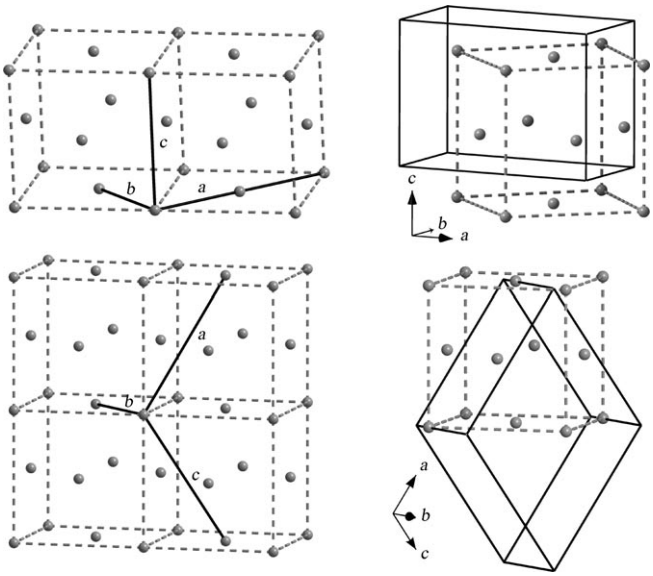

Figure 6. Above: geometrical relation between the orthorhombic axes and the orthorhombic unit cell of LT-Li_7PCh_6 with respect to a pseudocubic cell. Below: geometrical relation between the monoclinic axes and the monoclinic unit cell of LT-Li_6PS_5I with respect to a pseudocubic cell.

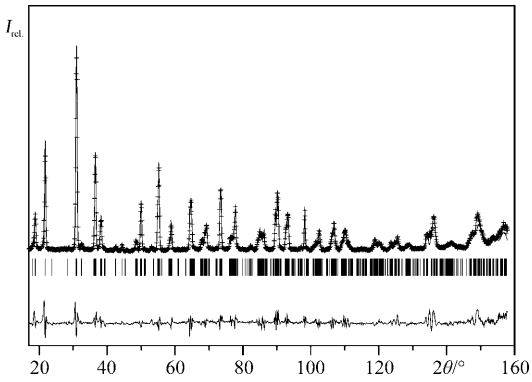

Figure 7. Rietveld refinement plot for Li_6PS_5I at 170 K (D1A, $\lambda = 1.91$ Å). Observed data (+), calculated pattern (solid line), and the difference between the two are shown (vertical bars (|) indicate the positions of Bragg reflections).

Table 5. Selected parameters and data for the Rietveld refinement of LT-Li_6PS_5I (neutron powder, 170 K).

formula	Li_6PS_5I	Z	4
T [K]	170	2θ range [°]	17.0–157.9
λ [Å]	1.91	background function	polynomial
crystal system	monoclinic	coefficients	4
space group	Cc	w_{RP} (fitted)	0.091
a [Å]	12.3217(4)	w_{RP} (background)	0.233
b [Å]	7.1377(3)	R_P (fitted)	0.070
c [Å]	12.4490(4)	R_P (background)	0.251
β [°]	109.481(3)	$\chi 2$	11.711
V [Å^3]	1032.19(6)		

Table 6. Atomic coordinates (all atoms on Wyckoff position 4*a*) and isotropic thermal displacement factors (U_{iso}) of LT-Li_6PS_5I (neutron powder; 170 K, fixed parameters without standard deviations, all positions fully occupied).

Atom	x	y	z	U_{iso} [Å^3]
Li1	0.985(5)	0.305(6)	0.371(5)	0.018(4)
Li2	0.765(5)	1.017(8)	0.885(4)	0.018(4)
Li3	0.830(4)	0.515(7)	0.385(4)	0.018(4)
Li4	0.709(4)	0.74(1)	0.066(4)	0.018(4)
Li5	0.980(5)	0.953(7)	0.131(4)	0.018(4)
Li6	0.997(5)	0.415(7)	0.679(4)	0.018(4)
P1	0.74700	0.743(4)	0.62400	0.008(2)
S1	0.691(3)	0.983(5)	0.672(3)	0.002(2)
S2	0.685(3)	0.480(5)	0.180(3)	0.002(2)
S3	0.921(2)	0.248(6)	0.174(3)	0.002(2)
S4	0.692(3)	0.734(5)	0.444(2)	0.002(2)
S5	0.872(4)	0.248(6)	0.490(3)	0.00253
I1	−0.004(3)	0.747(3)	0.371(2)	0.015(2)

Table 7. Selected interatomic distances in [Å] for LT-Li_6PS_5I (neutron powder; 170 K). (The **bold** entries refer to Li atoms with tetrahedral coordination.)

Li1–S3	2.35(7)	**Li4–S5**	**2.49(8)**
Li1–S4	2.46(7)	**Li4–I1**	**2.92(5)**
Li1–S5	2.38(9)	Li5–S2	2.40(7)
Li1–I1	3.16(5)	Li5–S3	2.35(7)
Li2–S1	2.51(6)	Li5–S5	2.31(6)
Li2–S4	2.23(7)	Li5–I1	3.28(6)
Li2–S5	2.42(7)	**Li6–S1**	**2.47(7)**
Li2–I1	3.36(7)	**Li6–S3**	**2.57(7)**
Li3–S2	**2.59(5)**	**Li6–S5**	**2.63(6)**
Li3–S4	**2.59(7)**	**Li6–I1**	**2.66(6)**
Li3–S5	**2.27(6)**	P–S1	2.01(4)
Li3–I1	**2.68(6)**	P–S2	1.99(4)
Li4–S1	**2.42(8)**	P–S3	2.02(2)
Li4–S2	**2.42(8)**	P–S4	2.11(2)

preference of Li^+ ions for a higher coordination number when compared to Cu^+. Surprisingly, the unit cell volume of LT-Li_6PS_5I is more or less constant between 90 and 180 K. This is due to an "internal compensation", because the lattice constant a increases from 12.2815(7) Å (90 K) to 12.3217(4) Å (170 K), while c decreases from 12.5027(6) Å (90 K) to 12.4490(4) Å (170 K) with increasing temperature, whereas b is more or less constant (see Figure 9 and Supporting Information). This behaviour nicely reflects the temperature-driven tendency of monoclinic (pseudocubic) LT-Li_6PS_5I towards cubic HT-Li_6PS_5I (Figure 9).

HT-$Li_{7-\delta}AsS_{6-\delta}X_\delta$ (X=Br, I) and HT-$Li_{7-\delta}AsSe_{6-\delta}I_\delta$: Single-crystal investigations of the first arsenic-containing Li argyrodites $Li_{7-\delta}AsS_{6-\delta}X_\delta$ (X = Br, I) and $Li_{7-\delta}AsSe_{6-\delta}I_\delta$ prove that Li_6AsS_5I and Li_6AsSe_5I exhibit an ordered anion partial structure with a full occupancy of iodine on the crystallographically independent positions Ch3 (same position as I in Li_6PS_5I). A refinement using the atomic form factors of S/Se on positions Ch1 and Ch2 shows for both compounds within the threefold standard deviation a full occupancy by S/Se. For $Li_{6.02}AsS_{5.02}Br_{0.98}$ a mixed occupancy of S/Br on the positions Ch2 and Ch3 is observed, whereas Ch1 (forming the

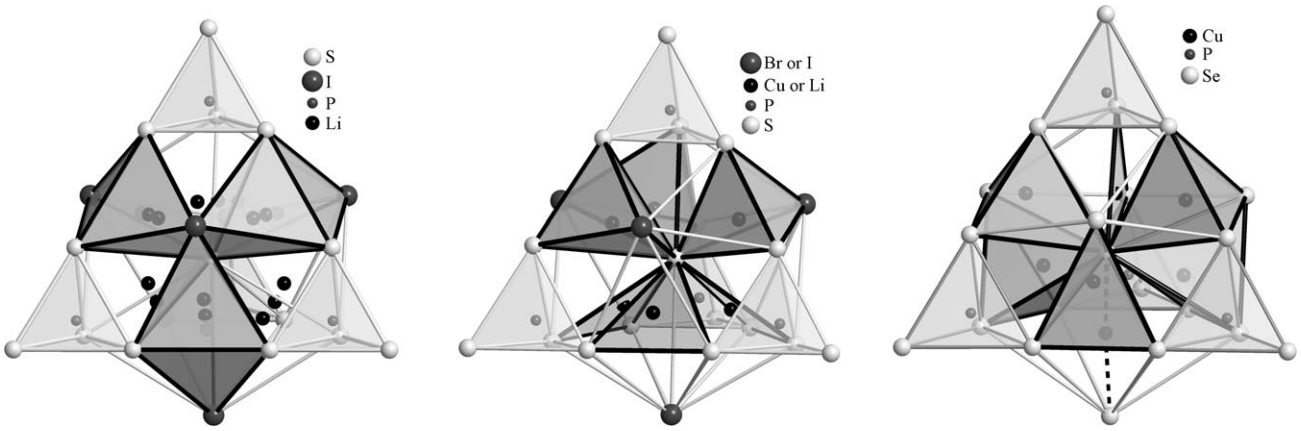

Figure 8. The $ChCh_{16}$ Frank–Kasper polyhedra around Ch2 with four attached PCh_4 tetrahedra (light gray) illustrating the different types of order/disorder observed for Li (Ag, Cu) atoms in argyrodites. Left: HT-Li_6PS_5I with Li^+ disordered over T5/T5a (for clarity, only three of the six T5 double tetrahedra are shown, and the "disordered" are illustrated as atom pairs). Middle: LT-Cu_6PS_5Br and LT-Li_6PS_5I (*Cc*, Cu^+/Li^+ ordered in T5 (3×) and T5a (3×)). Right: LT-Cu_7PSe_6 ($Pna2_1$, Cu ordered in T5 (5×), T5a (1×) and one linear coordinated position (dashed line)).

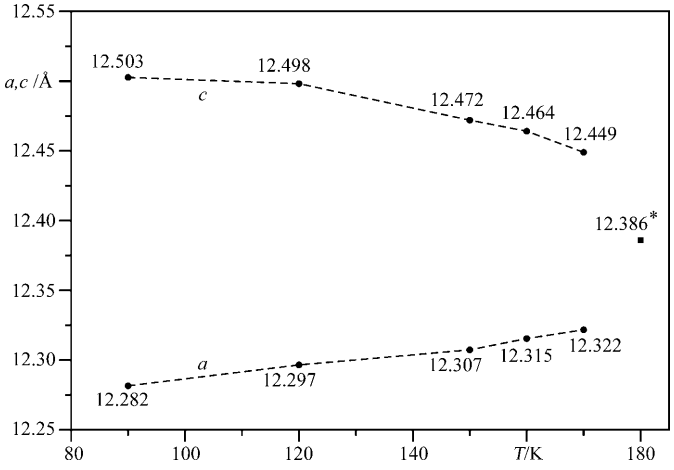

Figure 9. Temperature dependence of the lattice constants *a* and *c* for LT-Li_6PS_5I (from neutron powder data). *Value resulting from the cubic phase at 180 K for pseudo-monoclinic *a*/*c* lattice constants (see also Figure 6).

Table 8. Wyckoff positions (Wyck.), atomic coordinates, equivalent isotropic displacement parameters U_{eq} [Å^2], and occupancy (Occ.) [Å] for $Li_{6.02}AsS_{5.02}Br_{0.98}$, Li_6AsS_5I, and Li_6AsSe_5I.

	Wyck.	*x*	*y*	*z*	U_{eq} [Å^2]	Occ.
Li_6AsS_5I						
Li1	48*h*	0.285(2)	0.022(4)	0.715(2)	0.06(1)	0.52(8)
As1	4*b*	1/2	*x*	*x*	0.0179(5)	1
S1	16*e*	0.1218(1)	*x*	*x*	0.0254(6)	1
S2	4*d*	3/4	*x*	*x*	0.022(1)	1
I1	4*a*	0	*x*	*x*	0.0365(6)	1
$Li_{6.02}AsS_{5.02}Br_{0.98}$						
Li1	48*h*	0.295(1)	0.020(3)	0.705(1)	0.079(7)	0.55(3)
As1	4*b*	1/2	*x*	*x*	0.02237(2)	1
S1	16*e*	0.1231(1)	*x*	*x*	0.0317(4)	1
S2	4*d*	3/4	*x*	*x*	0.0275(7)	0.928(7)
Br2	4*d*	3/4	*x*	*x*	0.0275(7)	0.072(7)
S3	4*a*	0	*x*	*x*	0.0477(5)	0.082(9)
Br1	4*a*	0	*x*	*x*	0.0477(5)	0.918(9)
Li_6AsSe_5I						
Li1	48*h*	0.293(2)	0.020(3)	0.708(2)	0.07(1)	0.55(6)
As	4*b*	1/2	*x*	*x*	0.0145(3)	1
Se1	16*e*	0.1252(4)	*x*	*x*	0.0269(3)	1
Se2	4*d*	3/4	*x*	*x*	0.0194(3)	1
I1	4*a*	0	*x*	*x*	0.0385(3)	1

AsS_4 tetrahedra) remains unsubstituted. Similar to the case in P-containing $Li_{7-\delta}PCh_{6-\delta}X_\delta$, the halogen atoms substitute preferably the Ch3 position (Table 8). For all As argyrodites only one Li position with a significant delocalised electron density in the tetrahedra T5 (48*h*) can be refined (Table 8). A summary of the data collection and refinement details is given in Table 9. Selected distances are listed in Table 10.

LT-$Li_{7-\delta}AsS_{6-\delta}X_\delta$ (X=Br, I) and LT-$Li_{7-\delta}AsSe_{6-\delta}I_\delta$: As observed for Li_6PS_5I, the As-containing compound Li_6AsS_5I also shows a phase transition. The transition temperature was measured by DSC (T_t=173 K, reversible) and the transition was confirmed by powder X-ray data (T=113 K). An indexation of the X-ray powder diagram was successful (Table 1). The compound crystallises most likely in the monoclinic LT-Cu_6PS_5Br type. For $Li_{6.02}AsS_{5.02}Br_{0.98}$ and, surprisingly, also for the fully ordered Li_6AsSe_5I, no transition could be detected down to the experimental limit of 113 K in our laboratory.

Crystal chemical analysis and symmetry relation between the M^+ positions in HT and LT argyrodites based on the Frank–Kasper model: As mentioned above, the comparison between published structure data on HT and LT argyrodites suffers from different origin settings (Table 2). This is especially true for LT argyrodites, where the common cubic cell as reference is missing. A simple and fast method to overcome these problems is based on one of the Frank–Kasper polyhedra constituting the chalcogen (Ch) partial structure (neglecting Li and P). In each cubic HT argyrodite structure,

Table 9. Summary of data collection and refinement details for HT-Li_6AsS_5I, $Li_{6.02}AsS_{5.02}Br_{0.98}$, and Li_6AsSe_5I.

	Li_6AsS_5I	$Li_{6.02}AsS_{5.02}Br_{0.98}$	Li_6AsSe_5I
M_r [g mol^{-1}]	403.76	356.77	638.3
crystal system	cubic	cubic	cubic
space group	$F\bar{4}3m$	$F\bar{4}3m$	$F\bar{4}3m$
Z	4	4	4
crystal size [mm^3]	$0.1\times0.11\times0.12$	$0.08\times0.08\times0.09$	$0.04\times0.1\times0.38$
a [Å]	10.237(1)	10.101(1)	10.652(1)
V [Å^3]	1072.7(2)	1030.7(2)	1208.5(2)
ρ_{calcd} [g cm^{-3}]	2.50	2.29	3.51
μ [mm^{-1}]	6.944	8.109	20.358
$F(000)$	736	664	1096
T [K]	$T=293$	$T=293$	$T=293$
θ range [°]	3.45–30.36	3.5–30.16	3.31–30.25
index ranges	$-12\le h\le14$	$-14\le h\le14$	$-15\le h\le14$
	$-14\le k\le14$	$-13\le k\le12$	$-13\le k\le13$
	$-13\le l\le14$	$-14\le l\le14$	$-13\le l\le15$
measured reflections	3259	3142	2563
independent reflections	202	194	226
completeness to θ [%]	100	100	100
R_{int}	0.0512	0.0477	0.0357
data/restraints/parameter	202/0/12	194/0/14	226/0/12
R values [$I\ge2\sigma(I)$]	$R_1=0.037$, $wR_2=0.0948$	$R_1=0.0393$, $wR_2=0.0836$	$R_1=0.023$, $wR_2=0.0531$
R values (all data) R_1/wR_2	0.0413/0.0970	0.0399/0.0839	0.0244/0.0534
weighting scheme[a]	0.0623	0.0249	0.0334
goodness-of-fit	1.148	1.216	1.237
ρ_{max}/ρ_{min} [e Å^{-3}]	1.335/−1.024	1.224/−0.705	0.979/−0.433

[a] $w=1/[\sigma^2(F_o^2)+(AP)^2+BP]$, $P=(F_o^2)+2F_c^2)/3$.

Table 10. Comparison of selected distances [Å] for Li_6AsSe_5I, Li_6AsS_5I, and $Li_{6.02}AsS_{5.02}Br_{0.98}$.

	Li_6AsSe_5I	Li_6AsS_5I	$Li_{6.02}AsS_{5.02}Br_{0.98}$
Li–Ch1 (2×)	2.5198(2)	2.4253(2)	2.4059(2)
Li–Ch2 (2×)	2.5275(3)	2.3854(3)	2.4134(3) (S2/Br2)
Li–I1 (1×)	3.1344(2)	3.1181(3)	2.9317(2) (S3/Br1)
As–Ch1 (4×)	2.3091(8)	2.1595(1)	2.1534(2)
Li–Li (1×)	1.2781(1)	1.0191(1)	1.2930(1)

Ch1 defines *one* type of icosahedron (CN = 12), whereas Ch2 and Ch3 define two types of Friauf polyhedra (CN = 16). The two types of Friauf polyhedra can be distinguished by the number of attached PCh_4 tetrahedra (six or four). The one with four attached PCh_4 contains a representative set of independent Li positions. The specific Friauf polyhedron can also be identified easily in the LT modifications (in which more than three independent anion positions occur).

A few illustrative examples are given in Figure 8. The Friauf polyhedron centred at Ch2 in the HT modification (Figure 8) contains six T5 double tetrahedra (Table 3) and additionally twelve T2 tetrahedra. In HT-Li_6PS_5I, the 24 Li atoms per unit cell (six independent crystallographic positions) are statistically disordered over the two Wyckoff positions T5 (48*h*), and T5a (24*g*, Figure 8, left). In LT-Li_6PS_5I (or LT-Cu_6PS_5Br) the 24 Li^+ (Cu^+) ions are located in T5 (3×) and T5a (3×) (Figure 8, middle) in an ordered manner. In LT-Li_7PCh_6 (or LT-Cu_7PSe_6), the T5 double tetrahedra do not offer a sufficient number of positions for all 28 Cu atoms (seven independent crystallographic positions), because each T5 or T5a position can only be occupied by one Li^+ (Cu^+) at the same time (Figure 8, right). Thus, the seven Li atoms occupy 5×T5 and 1×T5a positions and an additional twofold coordinated position on a common edge of three T5 tetrahedra.

Experimental Section

All experiments were carried out in a glovebox under dry argon (Unilab, MBraun; H_2O <1 ppm, O_2 <1 ppm). The typical synthesis procedures are given below. The typical weight for the sum of all starting materials was about 0.25 g.

Synthesis of Li_7PCh_6 (Ch=S, Se): Li_2S was prepared by reaction of finely dispersed LiOH (Fluka) with H_2S at 573 K for 30 min.[18] Compounds Li_7PCh_6 (Ch = S, Se) were prepared by the reactions of Li_2S (3.21 mmol) with P_2S_5 (0.46 mmol; Acros 98+%), and Li_2Se (1.58 mmol; Cerac 99.5%) with P_2Se_5 (0.23 mmol, prepared by a published procedure[19]), respectively. The intimately mixed starting compounds were pressed into pellets (diameter: 6 mm or 10 mm), then placed into a graphitised quartz ampule. Subsequently, the ampule was sealed and heated to 923 K for one week in a tube oven. After completion of the reaction, the oven was slowly cooled down to room temperature at a cooling rate of 30 K h^{-1}. The products consisted of air-sensitive, colourless (S compound) or orange (Se compound) crystals.

Synthesis of $Li_{7-\delta}PCh_{6-\delta}X_\delta$ (Ch=S, Se; X = Cl, Br, I): $Li_{7-\delta}PCh_{6-\delta}X_\delta$ were synthesised from stoichiometric ratios of Li_2S,[18] P_2S_5 (Acros, 98+%), and LiX (Fluka, p.a.), or Li_2Se (Cerac, 99.5%), P_2Se_5,[19] and LiX (Fluka, p.a.), respectively. The synthetic procedure was similar to that used for Li_7PCh_6 (see above), except that the reaction was carried out at 823 K.

Synthesis of $Li_{7-\delta}AsS_{6-\delta}X_\delta$ (Ch=S; X=Br, I) and Li_6AsSe_5I: $Li_{7-\delta}AsS_{6-\delta}X_\delta$ and Li_6AsSe_5I were synthesised from Li_2S[18]/Li_2Se (Cerac 99.5%), As (Chempur, 99%), S (Chempur, 99.99%)/Se (Fluka, 99.99%), and LiX (Fluka, p.a.). The synthetic procedure was similar to that used for Li_7PCh_6 (see above), except that the reaction was carried out at 823 K.

Powder X-ray measurements: The air-sensitive products were prepared in a glovebox. The samples were ground and loaded with grease (Lithelen) between two Mylar foils (diameter: 0.1 mm). The diffraction data were collected on a Siemens D5000 diffractometer ($Cu_{K\alpha1}$ radiation, Ge monochromator). The data analyses were performed by using the STOE Software package WINXPOW.[20]

Neutron powder diffraction: Neutron powder diffraction data were collected on the high-resolution two-axis diffractometer D1A (ILL Grenoble; $\lambda=1.91$ Å) at different temperatures. For the Rietveld refinement, the program package FULLPROF[21] was used. The structure data of LT-Cu_6PS_5Br[5] were used as starting parameters.

Single-crystal investigations: Crystals of HT-$Li_{6.02}AsS_{5.02}Br_{0.98}$, HT-$Li_6AsS_5I$, HT-$Li_6AsSe_5I$, HT-$Li_6PSe_5I$, and HT-$Li_6PSe_5Cl$ of appropriate size were selected in a glovebox equipped with a microscope, and transferred into capillaries that were finally sealed. The capillaries were mounted on an imaging plate diffraction system (STOE IPDS I) and measured by using graphite monochromatised $Mo_{K\alpha}$ radiation ($\lambda=0.71073$ Å). The STOE IPDS program package[22] was used for data evaluation. For structure solution and refinement the programs SHELXS-

97[23] and SHELXL-97[23] were used. The analysis of the collected data with the programs RECIPE and SPACE[22] showed for Li_6AsSe_5I the presence of two domains, which were unsystematically intergrown. With the program TWIN,[22] overlapping reflections were rejected and the data of the major domain were used for the structure solution and refinement.

Further details of the crystal structure investigations may be obtained from the Fachinformationszentrum Karlsruhe, 76344 Eggenstein-Leopoldshafen, Germany (fax: (+49) 7247-808-666; e-mail: crysdata@fiz-karlsruhe.de) on quoting the depository numbers CSD-421210 (Li_6PSe_5I), CSD-421209 (Li_6PSe_5Cl), CSD-421083 (LT-Li_6PS_5I), CSD-380390 (Li_6AsSe_5I), CSD-380389 (Li_6AsS_5I), and CSD-380388 ($Li_{6.02}AsS_{5.02}Br_{0.98}$).

Thermal analysis: Differential scanning calorimetry measurements were performed on samples in stainless steel crucibles under a nitrogen atmosphere between 143 and 873 K with a heating rate of 7 K min^{-1} by using a Setaram DSC131. The preparation of the sealed crucible was carried out in an argon-filled glovebox. Differential thermal analyses were carried out in evacuated graphitised quartz ampules between room temperature and 673 K with a heating rate of 5 K min^{-1} by using a DTA-L62 (Linseis company).

Molecular dynamic simulations: Separate 15 ns molecular dynamics runs at 500 K and 1 atm were performed for Li_7PS_6 and Li_6PS_5I. Each compound was modeled by a $4\times4\times4$ supercell and empirical interaction potentials.[24] For constant-temperature and constant-pressure molecular dynamics simulations, a time step of 2 fs was used and Ewald summation was applied. Before the production runs, each model was allowed to relax for 1 ns. The occupancy of the different sites was evaluated on the basis of S···Li and I···Li contacts for which a cut-off distance of 2.5 Å was found to be suitable. Several simulation temperatures were tested. At temperatures large enough to allow reasonable sampling of all interstitial positions, thermal motion prevents a clear discrimination of the triangular coordination (type 5a) and the type 5 tetrahedra. Both were hence grouped as a single coordination type and taken as the reference state for performing the Boltzmann statistics.

Acknowledgements

The authors would like to thank the Deutsche Forschungsgemeinschaft for continuous financial support (DE 365/12-1).

[1] H.-J. Deiseroth, S.-T. Kong, H. Eckert, J. Vannahme, C. Reiner, T. Zaiß, M. Schlosser, *Angew. Chem.* **2008**, *120*, 767–770; *Angew. Chem. Int. Ed.* **2008**, *47*, 755–758.
[2] H.-J. Deiseroth, S. T. Kong, M. Schlosser, C. Reiner (University of Siegen), DE-102007048289A1, **2009**.
[3] M. Evain, E. Gaudin, F. Boucher, V. Petricek, F. Taulelle, *Acta Crystallogr. Sect. B* **1998**, *54*, 376–383.
[4] T. Zaiss, PhD Thesis, University of Siegen (Germany), **2005**.
[5] A. Haznar, A. Pietraszko, I. P. Studenyak, *Solid State Ionics* **1999**, *119*, 31–36.
[6] M. Onoda, X.-A. Chen, K. Kato, A. Sato, H. Wada, *Acta Crystallogr. Sect. B* **1999**, *55*, 721–725.
[7] B. Krebs, J. Mandt, *Z. Naturforsch. B* **1977**, *32*, 373–379.
[8] J. P. Deloume, R. Faure, H. Loiseleur, M. Roubin, *Acta Crystallogr. Sect. B* **1978**, *34*, 3189–3193.
[9] A. Weisbach, *Neues Jahrb. Mineral. Geol. Palaentol. Ref.* **1886**, II. Band, 67–71.
[10] C. Winkler, *Chem. Ber.* **1886**, *19*, 210–211.
[11] J.-F. Brice, *C. R. Seances Acad. Sci. Ser. C* **1976**, *283*, 581–584.
[12] H. Eckert, Z. Zhang, J. H. Kennedy, *Chem. Mater.* **1990**, *2*, 273–279.
[13] R. H. P. Francisco, T. Tepe, H. Eckert, *J. Solid State Chem.* **1993**, *107*, 452–459.
[14] P. Bagnoud, P. Feschotte, *Z. Metallk.* **1978**, *69*, 114–120.
[15] J. V. Unterrichter, K.-J. Range, *Z. Naturforsch. B* **1978**, *33*, 866–872.
[16] E. Gaudin, F. Boucher, V. Petricek, F. Taulelle, M. Evain, *Acta Crystallogr. Sect. B* **2000**, *56*, 402–408.
[17] E. Gaudin, V. Petricek, F. Boucher, F. Taulelle, M. Evain, *Acta Crystallogr. Sect. B* **2000**, *56*, 972–979.
[18] K. Yamamoto, N. Ikeda (Furukawa CO LTD), EP-0802159, **1997**.
[19] T. J. McCarthy, M. G. Kanatzidis, *Inorg. Chem.* **1995**, *34*, 1257–1267.
[20] WINXPOW, Version 1.08, STOE & Cie GmbH, Darmstadt, **2000**.
[21] FullProf.2k (Version 4.40), J. Rodríguez-Carvajal, Laboratoire Léon Brillouin, Gif-sur-Yvette, **2008**.
[22] IPDS-Software, Version 2.93, STOE & CIE, Darmstadt, **1999**.
[23] G. M. Sheldrick, *Acta Crystallogr. Sect. A* **2008**, *64*, 112–122.
[24] A. K. Rappe, C. J. Casewit, K. S. Colwell, W. A. Goddard, III, W. M. Skiff, *J. Am. Chem. Soc.* **1992**, *114*, 10024–10035.

Received: September 7, 2009
Published online: January 11, 2010

